

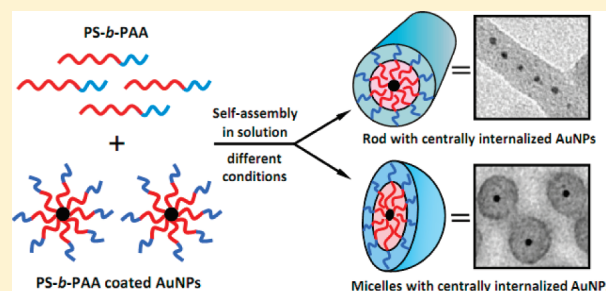
Controlled Incorporation of Particles into the Central Portion of Block Copolymer Rods and Micelles

Yiyong Mai and Adi Eisenberg*

Department of Chemistry, McGill University, 801 Sherbrooke Street West, Montreal, Quebec, H3A 2K6, Canada

Supporting Information

ABSTRACT: The controlled incorporation of preformed gold nanoparticles (AuNPs) into only the central portion of polystyrene₁₉₀-*block*-poly(acrylic acid)₂₀ (PS₁₉₀-*b*-PAA₂₀) block copolymer rods and micelles is described in this note. The strategy involves the formation of the rods or micelles in solution in the presence of AuNPs coated with PS₂₇₀-*b*-PAA₁₅ diblock copolymer. Statistical analysis shows that about 80% of the AuNPs are incorporated into the central ca. 4 vol % portion of the rods. The method does not require the block copolymers to bind, solvate, or otherwise interact during preparation with the ions of the metal involved, nor does it involve postassembly chemical reactions within the aggregates, and is thus suitable for a wide range of particles and block copolymer systems.



1. INTRODUCTION

Block copolymer aggregates formed by self-assembly of amphiphilic block copolymers (BCPs), including spheres, rods, and vesicles, among others, have attracted considerable interest not only for academic reasons, but also because of possible applications in fields such as medicine, electronics, and catalysis.^{1–31} For example, BCP rods, which have a hydrophobic cylindrical core and a hydrophilic corona surrounding the core, are a possible template for the preparation of rod- or wire-like metal materials^{26–30} as well as promising candidates as a drug delivery carrier.³¹

In recent years, many studies have focused on the incorporation of nanoparticles (NPs) into BCP aggregates, e.g., spherical micelles,^{32–35} lamellae or films,^{36–38} vesicles,^{39–45} tubules,^{46–48} and many others,^{49–51} since these hybrid aggregates may provide desirable properties in applications such as labeled materials, photonic nanodevices, or chemical sensors. However, only very few studies have been devoted to the incorporation of NPs into BCP rods; one of the difficulties encountered in rod incorporation is that the addition of NPs switches rods to lamellar structures.^{52,53} At present, successful approaches to achieve the incorporation of NPs into the cores of BCP rods involve two steps: adsorption of metal ions into rod cores, followed by postassembly chemical reactions. Several examples can be cited.^{54–57} Schmidt and co-workers incorporated HAuCl₄ in the core of a core–shell cylindrical polymer brush with a poly(2-vinylpyridine) (P2VP) core and a polystyrene (PS) shell; subsequent *in situ* reduction gave rise to gold nanowires within the P2VP cores.⁵⁴ Fahmi et al. incorporated HAuCl₄ into the cores of BCP rods formed by polystyrene-*block*-poly(4-vinylpyridine) (PS-*b*-P4VP) copolymers; the gold nanoparticles (AuNPs) were located throughout the P4VP cores after *in situ* reduction.⁵⁵ Winnik, Manners, and co-workers encapsulated silver NPs within

shell-cross-linked polyisoprene-*block*-polyferrocenyldimethylsilane (PI-*b*-PFS) rods using an *in situ* redox reaction between the electroactive PFS core and the incorporated silver ions; they observed, by dark-field technique of transmission electron microscopy (TEM), that most of the Ag NPs were positioned along the centerline of the rods.⁵⁶ Our group embedded Cd²⁺ ions into worm-like micelles formed by poly(ethylene oxide)-*block*-polystyrene-*block*-poly(acrylic acid) (PEO-*b*-PS-*b*-PAA) triblock copolymers; CdS NPs were formed inside the worm-like micelles after exposure of the Cd²⁺ ions to H₂S.⁵⁷ The above-mentioned methods are not suitable for preformed NPs, or rods made of BCPs incapable of binding, solvating, or otherwise incorporating metal ions. To the best of our knowledge, the controlled incorporation of preformed NPs into only the central portion of BCP rods has not been reported as yet.

By contrast to BCP rods, a number of attempts have succeeded in localizing preformed NPs in the central portion of spherical micelles. For instance, Kang and Taton localized AuNPs in the center of PS₂₅₀-*b*-PAA₁₃ micelles by adding water into the mixed DMF solution of preformed AuNPs, dodecanethiol, and PS₂₅₀-*b*-PAA₁₃ copolymer.³² Other examples can be found in the cited literature.^{33–35}

In a previous study, we developed an approach to incorporate preformed NPs into only the central portion of vesicle walls.⁴⁵ The strategy consists of two sequential steps. The first involves the stabilization of the NPs with diblock copolymers of the same or similar composition as the diblock used for the preparation of the vesicles; the second involves the formation of the vesicles in

Received: January 6, 2011

Revised: March 17, 2011

Published: March 28, 2011

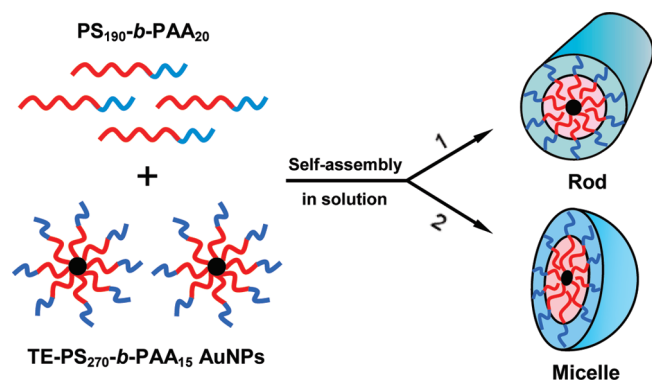


Figure 1. Schematic illustration of incorporation of diblock copolymer coated AuNPs into the central portion of BCP rods or micelles. The red color represents the hydrophobic PS composition (or the core in the rod or the micelle), and the blue color expresses the hydrophilic PAA composition (or the corona in the rod or the micelle, which cannot be seen in TEM images without staining). The numbers, 1 and 2, denote different conditions of self-assembly in solution. (1) The PS₁₉₀-*b*-PAA₂₀ copolymer and the AuNPs were simultaneously dissolved in DMF/H₂O (91/9, w/w) mixed solvent; (2) 25 wt % water was added dropwise into DMF solution of the PS₁₉₀-*b*-PAA₂₀ copolymer and the AuNPs.

the presence of the diblock copolymer coated NPs in solution. This method does not involve postassembly chemical reactions within the aggregates, and is thus expected to be suitable for a wide range of NPs and BCP systems. In the present work, we extend this method to BCP rods and micelles. The PS₁₉₀-*b*-PAA₂₀ copolymer was used as either a rod or micelle former, depending on the specific self-assembly conditions; the AuNPs coated with the PS₂₇₀-*b*-PAA₁₅ diblock copolymer (named TE-PS₂₇₀-*b*-PAA₁₅ AuNPs, TE represents a thiocysteine end group⁴⁵) were the species to be incorporated, as is illustrated in Figure 1 (to be discussed in detail later). TEM micrographs show that the AuNPs are selectively localized in the central portion of the BCP rods or micelles. The present work is a continuation of the previous study on incorporation of pre-formed NPs into only the central portion of vesicle walls, and illustrates the applicability of the method to BCP aggregates of other morphologies as well. It is reported in a separate note because of the high precision of the central localization, in that ca. 80% of the preformed NPs are located in the central ca. 4 vol % of the rods, an unprecedented level of control.

2. EXPERIMENTAL SECTION

The experimental details are given in the Supporting Information.

3. RESULTS AND DISCUSSION

3.1. Incorporation of AuNPs into BCP Rods. The PS₁₉₀-*b*-PAA₂₀ copolymer was found to be a suitable material for the formation of BCP rods with an average diameter of ca. 30 nm in DMF/water (91/9, w/w) mixed solvent, as described in previous work from this group.²⁷ TE-PS₂₇₀-*b*-PAA₁₅ AuNPs have an average gold particle size of 4.0 ± 0.7 nm, and the average number of the TE-PS₂₇₀-*b*-PAA₁₅ chains coated on one AuNP is ca. 90.⁴⁵ In the present work, the incorporation of AuNPs into BCP rods was carried out by simultaneously dissolving the PS₁₉₀-*b*-PAA₂₀ copolymer and the TE-PS₂₇₀-*b*-PAA₁₅ AuNPs in the DMF/water (91/9, w/w) mixed solvent. The initial weight

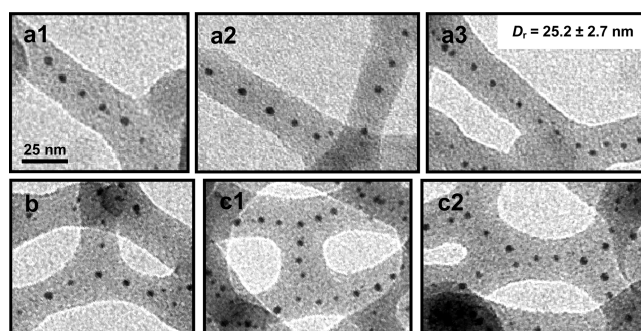


Figure 2. Typical TEM images of BCP rods with internalized AuNPs prepared from 1:2 (w/w) DMF/H₂O mixed solution of the TE-PS₂₇₀-*b*-PAA₁₅ AuNPs and the PS₁₉₀-*b*-PAA₂₀ copolymer. Key: (a) straight rods; (b) Y-junction; (c) rodlike aggregates with increased defect density.

ratio of the TE-PS₂₇₀-*b*-PAA₁₅ AuNPs to the PS₁₉₀-*b*-PAA₂₀ copolymer in the mixed solution was 1:2 (0.25 wt %/0.5 wt %) or 1:5 (0.1 wt %/0.5 wt %). Other weight ratios were not explored. Figure 2 shows typical TEM images of the BCP rods or rodlike aggregates, including straight rods, Y-junction, and rodlike aggregates with increased defect density, prepared from the 1:2 (w/w) solution of the AuNPs and the PS₁₉₀-*b*-PAA₂₀ copolymer. For convenience, in the following text we refer to the rodlike aggregates as rods as well. The average diameter (D_r) of the rods is 25.2 ± 2.7 nm. In the TEM images, such as those in Figure 2, a number of AuNPs can be seen in the rods. Most importantly, for all the rods in the TEM images, the AuNPs are seen clearly to be localized only in the central portion of the rods. Tilting studies in TEM confirm that the observed central localization of the AuNPs in the rods is independent of the orientation of the rods (see Figure S1 in the Supporting Information). By contrast, if the AuNPs had been randomly distributed within the rods⁵⁵ or had been located on the interfaces of the rods,⁵⁸ they would be seen everywhere in the rods in the TEM images, i.e., the sections near the interfaces of the rods would also contain AuNPs; clearly, these sections appear empty in the TEM images in the present work.

It is noted that parts b and c of Figure 2 show some AuNPs in the junction centers of Y- or T-junctions, which are considered to be energetically unfavorable. Similar observations have been also made by Listak and Bockstaller in BCP/NP blend lamella systems.³⁸ It should be mentioned here, that in the rods prepared in the absence of AuNPs, the Y- or T-junction defects are found as well, but the number density of the defects is lower than that in the rods containing AuNPs. The increased defect density in the rods containing AuNPs indicates that the addition of particles might stabilize the formation of the Y- or T-junctions in the rods under our experimental conditions.

On the basis of the TEM results, it is useful to recall the schematic diagram on the upper right side of Figure 1, which illustrates a probable mode of the rod incorporation. It shows the situation of each AuNP located in the central portion of the rod, with the coated chains (PS-*b*-PAA) extended toward the outside of the rod. The aggregates in the rod are drawn with the hydrophilic segments of the protective diblocks in the water phase, along with the hydrophilic segments of the unattached rod forming diblocks. In addition, it can be calculated that the freely jointed length of a chain of 270 repeat units (as in TE-PS₂₇₀-*b*-PAA₁₅ AuNPs) is ca. 3 nm, while the fully stretched length of the PS block is ca. 68 nm. It should be recalled that the average size of the AuNPs is ca. 4 nm, while the average diameter of the rod

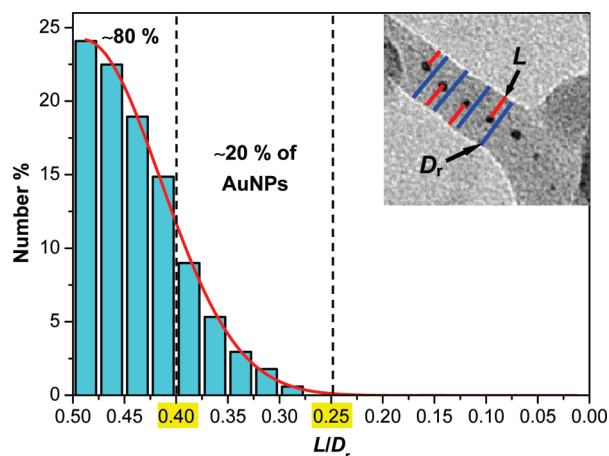


Figure 3. Radial distribution of the AuNPs in the BCP rods. The inset shows the schematic illustration of measuring the distances (L) of each AuNP to the nearest point on the closer edge of the rod (indicated by the red line), and the diameters (D_r) of the corresponding parts of the rods (indicated by the blue line) in TEM images.

cores is ca. 25 nm. Thus, the distance that the PS blocks on the NPs in the rods have to span is ca. $(25 - 4)/2 \approx 11$ nm, which is between the freely jointed length and the fully stretched length of the PS blocks on the AuNPs. This distance appears reasonable. Finally, incorporation involving a noncentral localization would involve a highly unfavorable entropy term in the free energy, since the attached chains would have to be distributed nonuniformly around the particle. Therefore, in view of the reasons mentioned above, if the AuNPs are incorporated into the rods, it is reasonable to expect that the AuNPs should be located in the central portion of the rods in the mode shown in the upper right corner of Figure 1.

To ascertain to what extent the central localization of the AuNPs in the rods is supported by TEM, we measured the distances of each AuNP to the nearest point on the closest edge of the rods (L , indicated by the red line in the inset of Figure 3), along with the diameters of the corresponding parts of the rods (D_r , indicated by the blue line) in TEM images. A plot of the distribution of the distance to diameter ratios (L/D_r) is shown in Figure 3. It can be calculated that about 80% of the AuNPs are localized in the central ca. 20% ($(0.5 - 0.4) \times 2$ on the L/D_r axis in Figure 3) linear portion of the rod diameter, i.e. central ca. 4% (0.2×0.2) portion of the cross-sectional area of the rods, or central ca. 4 vol % portion of the rods; all the AuNPs are located in the central ca. 50% ($(0.5 - 0.25) \times 2$) linear portion of the rods, i.e. central ca. 25 vol % (0.5×0.5) portion of the rods.

Finally, it should be mentioned that, when the initial weight ratio of the AuNPs to the PS₁₉₀-*b*-PAA₂₀ copolymer in the original mixed solution was decreased from 1:2 to 1:5, BCP rods with the centrally localized AuNPs were obtained as well, but the number density of the AuNPs in the rods decreased and a few “empty” rods (without AuNPs) appeared. The distribution histograms of the interparticle distances of the adjacent AuNPs along the rods are shown in Figure S2 in the Supporting Information, which statistically indicates the reduction of the number density of the AuNPs in the rods with decreasing initial weight ratio of the AuNPs to the PS₁₉₀-*b*-PAA₂₀ copolymer; more details about the distribution histograms are given in the caption of Figure S2. At present, we do not have sufficient data to quantify the relationship between the number density of the

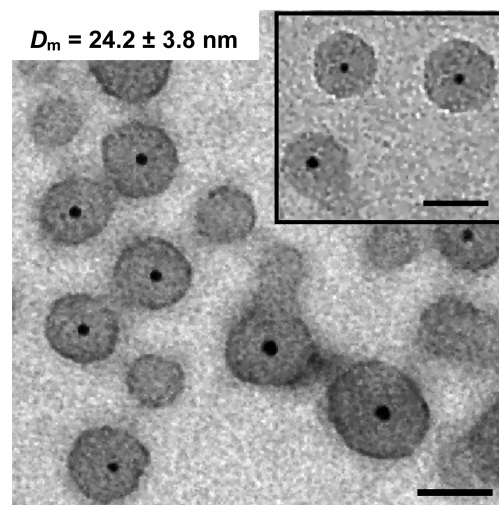


Figure 4. Typical TEM image of the micelles prepared from 1:1 (w/w) DMF solution of the PS₁₉₀-*b*-PAA₂₀ copolymer and the TE-PS₂₇₀-*b*-PAA₁₅ AuNPs. The micelles were stained by dilute CsOH solution to enhance edge contrast. The inset shows the unstained micelles at a different magnification. The D_m of the stained micelles and that of the unstained ones are very close. The scale bars represent 25 nm.

AuNPs in the rods and the initial weight ratio of the AuNPs to the PS₁₉₀-*b*-PAA₂₀ copolymer.

3.2. Incorporation of AuNPs into BCP Micelles. Empty micelles were prepared by the dropwise addition of water into the 0.5 wt % DMF solution of only the PS₁₉₀-*b*-PAA₂₀ copolymer. The average diameter of the micelles is 24.3 ± 3.6 nm. By contrast, when water was added dropwise into the 0.5 wt % DMF solution of only the TE-PS₂₇₀-*b*-PAA₁₅ AuNPs, precipitates along with some large compound micelles of ca. 124 ± 81 nm were observed. It should be pointed out here that we did not intend to maximize the coating when we prepared the TE-PS₂₇₀-*b*-PAA₁₅ AuNPs; thus the lack of sufficient polymer chains stabilizing the AuNPs or the small hydrophilic fraction of PS₂₇₀-*b*-PAA₁₅ might cause the precipitation after the addition of water; on the other hand, the incomplete coating on the AuNPs would leave space for a number of PS-*b*-PAA chains that are not chemically anchored to the metal surface, but held primarily by hydrophobic interactions with the bonded PS-*b*-PAA chains,³³ as is illustrated on the lower right side of Figure 1.

The incorporation of AuNPs into micelles was performed by dropwise addition of water into the 1:1 (0.5 wt %/0.5 wt %) DMF mixed solution of the TE-PS₂₇₀-*b*-PAA₁₅ AuNPs and the PS₁₉₀-*b*-PAA₂₀ copolymer. Other weight ratios were not explored. In this case, no precipitate was found after the addition of water; this might be attributed to the formation of micelles by the TE-PS₂₇₀-*b*-PAA₁₅ AuNPs and the PS₁₉₀-*b*-PAA₂₀ chains, which have a larger hydrophilic fraction compared with PS₂₇₀-*b*-PAA₁₅. Figure 4 shows a typical TEM image of the micelles prepared from the mixed solution, the average diameter (D_m) of the micelles with AuNPs is 24.2 ± 3.8 nm, very close to that of the rods (25.2 ± 2.7 nm). In all TEM images of the micelles, such as that in Figures 4, the AuNPs are clearly seen in the central portion of most micelles; some micelles do not contain AuNPs. Tilting TEM experiments also confirm that the observed central localization of the AuNPs in the micelles in TEM images is independent of the orientations of the micelles (see Figure S3 in the Supporting Information). In addition, the average aggregation

number of the PS₁₉₀-*b*-PAA₂₀ chains in an AuNP-containing micelle is estimated to be ca. 100; the detailed calculation is given on pages S4–S5 in the Supporting Information. At this point, one should recall the schematic illustration on the lower right side of Figure 1, which depicts the likely mode of the micelle incorporation. It shows that each AuNP is located in the central portion of the micelle, with the corona chains (PS-*b*-PAA) extended outward from the AuNP. The aggregate in the micelle is drawn with the hydrophilic segments of the protective diblocks in the water phase, along with the hydrophilic segments of the micelle forming diblocks. For these reasons, along with reasons similar to those described previously for rod incorporation, the AuNPs are believed to be localized in the central portion of the micelles as well.

4. CONCLUSIONS

This paper describes the controlled incorporation into the central portion of BCP rods or micelles of diblock copolymer coated AuNPs, which have a coating of a similar composition to that of the diblock used for the preparation of the BCP rods or micelles (Figure 1). TEM images (Figure 2 and Figure 4), together with TEM tilting experiments, demonstrate that the AuNPs are indeed localized only in the central portion of the rods or micelles. The radial distribution of the AuNPs in the rods (Figure 3) shows that about 80% of the AuNPs are localized in the central ca. 4 vol % portion of the rods. To our knowledge, this represents the most precise central localization of preformed NPs achieved to date

■ ASSOCIATED CONTENT

S Supporting Information. Experimental section, TEM images obtained from the tilting TEM experiments, and statistical distributions of the AuNPs along the rods, etc. This material is available free of charge via the Internet at <http://pubs.acs.org>.

■ AUTHOR INFORMATION

Corresponding Author

*E-mail: adi.eisenberg@mccgill.ca.

■ ACKNOWLEDGMENT

The authors would like to thank Dr. Lifeng Zhang for preparing the PS₁₉₀-*b*-PAA₂₀ copolymer, and thank Dr. Shaoyong Yu, Dr. Tony Azzam, and Mr. Georgios Rizis for useful suggestions and help in this work. The authors would also like to acknowledge financial support from the Natural Science and Engineering Research Council of Canada (NSERC).

■ REFERENCES

- (1) van Hest, J. C. M.; Delnoye, D. A. P.; Baars, M. W. P. L.; van Genderen, M. H. P.; Meijer, E. W. *Science* **1995**, *268*, 1592–1595.
- (2) Zhang, L. F.; Eisenberg, A. *Science* **1995**, *268*, 1728–1731.
- (3) Zhang, L. F.; Yu, K.; Eisenberg, A. *Science* **1996**, *272*, 1777–1779.
- (4) Liu, G. J. *Adv. Mater.* **1997**, *9*, 437–439.
- (5) Discher, B. M.; Won, Y. Y.; Ege, D. S.; Lee, J. C. M.; Bates, F. S.; Discher, D. E.; Hammer, D. A. *Science* **1999**, *284*, 1143–1146.
- (6) Chen, L.; Shen, H. W.; Eisenberg, A. *J. Phys. Chem. B* **1999**, *103*, 9488–9497.
- (7) Shen, H. W.; Eisenberg, A. *Angew. Chem., Int. Ed.* **2000**, *39*, 3310–3312.

- (8) Rosler, A.; Vandermeulen, G. W. M.; Klok, H. A. *Adv. Drug Delivery Rev.* **2001**, *53*, 95–108.
- (9) Ober, C. K. *Science* **2002**, *296*, 859–861.
- (10) Discher, D. E.; Eisenberg, A. *Science* **2002**, *297*, 967–973.
- (11) Jain, S.; Bates, F. S. *Science* **2003**, *300*, 460–464.
- (12) Riess, G. *Prog. Polym. Sci.* **2003**, *28*, 1107–1170.
- (13) Antonietti, M.; Förster, S. *Adv. Mater.* **2003**, *15*, 1323–1333.
- (14) Terreau, O.; Luo, L. B.; Eisenberg, A. *Langmuir* **2003**, *19*, 5601–5607.
- (15) Chen, D. Y.; Jiang, M. *Acc. Chem. Res.* **2005**, *38*, 494–502.
- (16) Mai, Y. Y.; Zhou, Y. F.; Yan, D. Y. *Macromolecules* **2005**, *38*, 8679–8686.
- (17) Li, Z.; Hillmyer, M. A.; Lodge, T. P. *Nano Lett.* **2006**, *6*, 1245–1249.
- (18) O'Reilly, R. K.; Hawker, C. J.; Wooley, K. L. *Chem. Soc. Rev.* **2006**, *35*, 1068–1083.
- (19) Mai, Y. Y.; Zhou, Y. F.; Yan, D. Y. *Small* **2007**, *3*, 1170–1173.
- (20) Kumar, M.; Grzelakowski, M.; Zilles, J.; Clark, M.; Meier, W. *Proc. Natl. Acad. Sci. U.S.A.* **2007**, *104*, 20719–20724.
- (21) Duncan, T. V.; Ghoroghchian, P. P.; Rubtsov, I. V.; Hammer, D. A.; Therien, M. J. *J. Am. Chem. Soc.* **2008**, *130*, 9773–9784.
- (22) Howse, J. R.; Jones, R. A. L.; Battaglia, G.; Ducker, R. E.; Leggett, G. J.; Ryan, A. J. *Nat. Mater.* **2009**, *8*, 507–511.
- (23) Yu, S. Y.; Azzam, T.; Rouiller, L.; Eisenberg, A. *J. Am. Chem. Soc.* **2009**, *131*, 10557–10566.
- (24) Blanz, A.; Armes, S. P.; Ryan, A. J. *Macromol. Rapid Commun.* **2009**, *30*, 267–277.
- (25) Kim, K. T.; Meeuwissen, S. A.; Nolte, R. J. M.; van Hest, J. C. M. *Nanoscale* **2010**, *2*, 844–858.
- (26) Won, Y. Y.; Davis, H. T.; Bates, F. S. *Science* **1999**, *283*, 960–963.
- (27) Zhang, L. F.; Eisenberg, A. *Macromolecules* **1999**, *32*, 2239–2249.
- (28) Liu, Y.; Abetz, V.; Müller, A. H. E. *Macromolecules* **2003**, *36*, 7894–7898.
- (29) Wang, X. S.; Guerin, G.; Wang, H.; Wang, Y. S.; Manners, I.; Winnik, M. A. *Science* **2007**, *317*, 644–647.
- (30) Zhong, S.; Cui, H. G.; Chen, Z. Y.; Wooley, K. L.; Pochan, D. J. *Soft Matter* **2008**, *4*, 90–93.
- (31) Cai, S. S.; Vijayan, K.; Cheng, D.; Lima, E. M.; Discher, D. E. *Pharm. Res.* **2007**, *24*, 2099–2109.
- (32) Kang, Y.; Taton, T. A. *Angew. Chem., Int. Ed.* **2005**, *44*, 409–412.
- (33) Azzam, T.; Eisenberg, A. *Langmuir* **2007**, *23*, 2126–2132.
- (34) Chen, T.; Yang, M. X.; Wang, X. J.; Tan, L. H.; Chen, H. Y. *J. Am. Chem. Soc.* **2008**, *130*, 11858–11859.
- (35) Li, D. X.; He, Q.; Li, J. B. *Adv. Colloid Interface Sci.* **2009**, *149*, 28–38.
- (36) Bockstaller, M. R.; Lapetnikov, Y.; Margel, S.; Thomas, E. L. *J. Am. Chem. Soc.* **2003**, *125*, 5276–5277.
- (37) Chiu, J. J.; Kim, B. J.; Kramer, E. J.; Pine, D. J. *J. Am. Chem. Soc.* **2005**, *127*, 5036–5037.
- (38) Listak, J.; Bockstaller, M. R. *Macromolecules* **2006**, *39*, 5820–5825.
- (39) Lecommandoux, S.; Sandre, O.; Chécot, F.; Rodriguez-Hernandez, J.; Perzynski, R. *Adv. Mater.* **2005**, *17*, 712–718.
- (40) Du, J. Z.; Tang, Y. Q.; Lewis, A. L.; Armes, S. P. *J. Am. Chem. Soc.* **2005**, *127*, 17982–17983.
- (41) Li, Y. T.; Smith, A. E.; Lokitz, B. S.; McCormick, C. L. *Macromolecules* **2007**, *40*, 8524–8526.
- (42) Binder, W. H.; Sachsenhofer, R.; Farnika, D.; Blaasb, D. *Phys. Chem. Chem. Phys.* **2007**, *9*, 6435–6441.
- (43) Krack, M.; Hohenberg, H.; Kornowski, A.; Lindner, P.; Weller, H.; Förster, S. *J. Am. Chem. Soc.* **2008**, *130*, 7315–7320.
- (44) Mueller, W.; Koynov, K.; Fischer, K.; Hartmann, S.; Pierrat, S.; Basche, T.; Maskos, M. *Macromolecules* **2009**, *42*, 357–361.
- (45) Mai, Y. Y.; Eisenberg, A. *J. Am. Chem. Soc.* **2010**, *132*, 10078–10084.
- (46) Yan, X. H.; Liu, G. J.; Li, Z. *J. Am. Chem. Soc.* **2004**, *126*, 10059–10066.

- (47) Wang, X. S.; Wang, H.; Coombs, N.; Winnik, M. A.; Manners, I. *J. Am. Chem. Soc.* **2005**, *127*, 8924–8925.
- (48) Lo, P. K.; Karam, P.; Aldaye, F. A.; McLaughlin, C.; Hamblin, G. D.; Cosa, G.; Sleiman, H. F. *Nature Chem.* **2010**, *2*, 319–328.
- (49) Balazs, A. C.; Emrick, T.; Russell, T. P. *Science* **2006**, *314*, 1107–1110.
- (50) Haryono, A.; Binder, W. H. *Small* **2006**, *2*, 600–611.
- (51) Mendoza, C.; Gindy, N.; Gutmann, J. S.; Fromsdorf, A.; Förster, S.; Fahmi, A. *Langmuir* **2009**, *25*, 9571–9578.
- (52) Thompson, R. B.; Ginzburg, V. V.; Matsen, M. W.; Balazs, A. C. *Science* **2001**, *292*, 2469–2472.
- (53) Lee, J. Y.; Shou, Z. Y.; Balazs, A. C. *Macromolecules* **2003**, *36*, 7730–7739.
- (54) Djalali, R.; Li, S.; Schmidt, M. *Macromolecules* **2002**, *35*, 4282–4288.
- (55) Fahmi, A.; Pietsch, T.; Mendoza, C.; Cheval, N. *Mater. Today* **2009**, *12*, 44–50.
- (56) Wang, H.; Wang, X. S.; Winnik, M. A.; Manners, I. *J. Am. Chem. Soc.* **2008**, *130*, 12921–12930.
- (57) Duxin, N.; Liu, F.; Vali, H.; Eisenberg, A. *J. Am. Chem. Soc.* **2005**, *127*, 10063–10069.
- (58) Zubarev, E. R.; Xu, J.; Sayyad, A.; Gibson, J. D. *J. Am. Chem. Soc.* **2006**, *128*, 15098–15099.